



Application of EMI Technique in Crack Propagation Under the Block Loading Conditions

Reetesh Kumar Shukla, Gurkirat Singh and K N Pandey

EasyChair preprints are intended for rapid dissemination of research results and are integrated with the rest of EasyChair.

May 5, 2022

Track1: Machine Design

Application of EMI Technique in Crack Propagation under the Block Loading Conditions

Reetesh Kumar Shukla¹, Gurkirat Singh² and K.N.Pandey³

¹Department of Mechanical Engineering, MN National Institute of Technology Allahabad
Prayagraj-211004, India

²Department of Mechanical Engineering, MN National Institute of Technology Allahabad
Prayagraj-211004, India

*Corresponding author: knpandey@mnnit.ac.in

Abstract

The behavior of a component under random loading conditions can be studied by converting the random loading into a block loading. Therefore, knowledge of initiation and propagation of a crack under block loading conditions is very important for the safety and reliability of a machine components and structures. In the present paper an experimental study has been made to monitor fatigue crack initiation and propagation under block loading conditions with the help of electromechanical impedance technique (EMI). A number of sequences of block loads were considered as variable amplitude loading. The piezoelectric sensor bonded on the Compact Tension (CT) specimen was used as a collocated actuator and sensor. The basic concept is to use simultaneously the high-frequency mechanical excitations and responses employing piezoelectric transducer to monitor the local change in mechanical impedance with respect to the applied cyclic loads. The change in mechanical impedance indicated the incipient damage. The impedance signature (conductance and susceptance) of specimen were recorded. The conductance (real part of admittance) signature is preferred as a damage identifier due to its higher sensitivity for damage in comparison to the susceptance signature.

Keywords: Block loading, EMI, Conductance, susceptance, Fatigue crack

1. Introduction

There is a phenomenal rise in failure of in-service components in the field of engineering in the recent years. Major components like ships, aeroplanes, dams are subjected to severe loading and their performance is likely to change with time. It is, therefore, necessary to check the performance of a machine component through continuous monitoring. Electro-mechanical impedance (EMI) technique, which is based on piezo-electric ceramic (PZT) sensors; operates at higher frequency range and can typically detect damage at microscopic level and at a very early stage. The application was recognised by Sun et al. [1] by applying the technique on a laboratory size truss which was later extended to large trusses by Ayres et al. [2]. Now the technique has been applied to applications ranging from civil structural components [3-5], bolted joint structure [6], high temperature components such as steam pipes and boilers in power plants [3-4], thin structural elements [7], aircraft components [8], and structures [9] etc. The EMI technique has been successfully applied to detect the presence of damage and to monitor its progress under fatigue loading [10-19] but mostly under constant amplitude loading conditions. Although there are many works related to determine the effect of block loading (load sequence) on life of a component [20-25] but EMI technique is not applied to monitor the damage. In the present paper, EMI technique is used to study the effect of load sequence on the life of a component

2 Material and experimental set-up

2.1 Specimen material and geometry

The material used for the study was Al-5083-O aluminium alloy with chemical composition and mechanical properties as shown in Table 1 and 2 respectively.

Table 1 Chemical composition of the materials by weight (%)

Material	Al	Cu	Mg	Mn	Cr	Si	Ti	Zn
Al-5083-O	92.4-95.6	0.1	4.0-4.5	0.4-1.0	0.05-0.25	0.40	0.15	0.25

Table 2 Mechanical properties of the materials

Material	Density	Modulus of elasticity	Ultimate strength	Poisson's ratio	Elongation at fracture
Al-5083-O	2.6 g/cc	70300 N/mm ²	315MPa	0.33	16%

Compact tension (CT) specimen of the selected material were prepared as per ASTM-E647 standard. It was a single edge-notch specimen of length, breadth and thickness equal to 48 mm, 46.5 mm, and 6.2 mm respectively, as shown in Figure (1a). Straight- notch was made on middle position of the specimen (Figure 1 (b)) with the help of wire EDM. The notch of the specimen was subjected to fatigue preloading to convert it into a sharp crack. For this, the maximum cyclic load of 4 kN was applied till a sharp crack was created of 1 mm length. After this, crack growth tests were performed till fracture of the specimen [26-28].

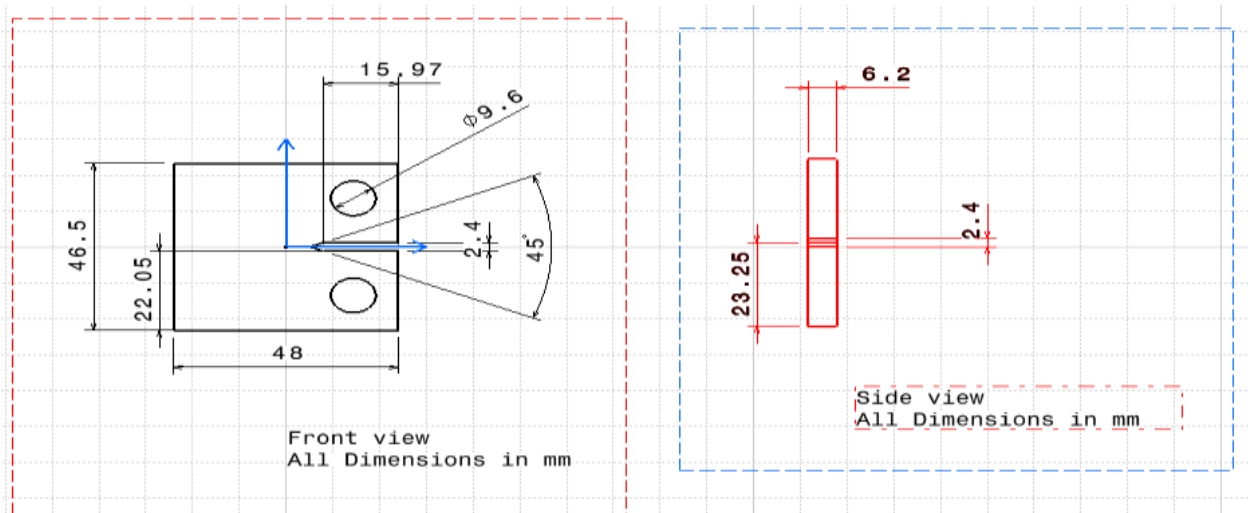


Figure 1 (a) Compact Tension (CT) specimen dimensions

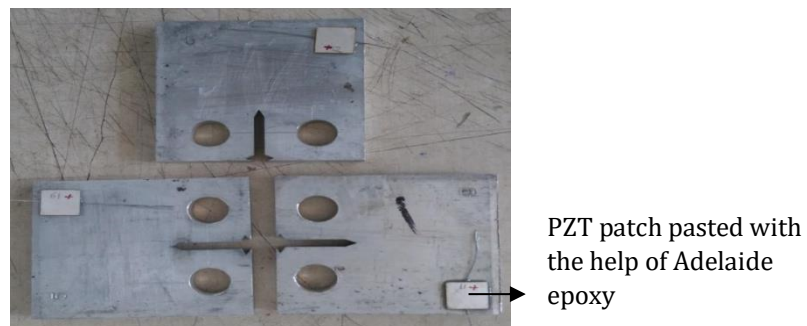


Figure 1 (b) CT specimen with surface bonded PZT patch

2.2 The piezo-electric sensor: PZT

The lead zirconate titanate, also called PZT, was taken as the piezo-electric sensor. It is inert to chemicals and exhibits a high sensitivity of about 3 $\mu\text{V}/\text{Pa}$, providing a sophisticated charge amplification capacity to cushion the high impedance generated by the source [29]. PZT patches of dimension 10mm \times 10mm \times 0.2

mm, were procured from Central Electronics Limited, Industrial Area, Sahibabad, Uttar Pradesh (India). These patches were PIC 151 compliance ceramic sensor. The PZT patch is protected against damage during sample preparation and testing by providing a protective layer of silicone rubber. The PZT sensor has a long range of linearity up to 2 kV/cm, quick response, long period stability and high efficiency of energy conversion. Physical, Electrical, and Mechanical properties of PZT patch are shown in Table 3.

Table 3 PZT patch properties [29-30]

S. No	Physical Parameter	Symbols	Value
1	Young's modulus at constant electric field	γE	$6.3 \times 10^{10} N/M^2$
2	Piezoelectric strain coefficient	d_{31}	$-166 \times 10^{-12} m/V$
3	Electric permittivity at constant stress	ϵ^T	$1.5 \times 10^{-8} Farad/m$
4	Density	ρ	$7650 kg/M^3$
5	Dielectric loss factor	δ	.012
6	Mechanical loss factor	\aleph	.001
7	Thickness of PZT patch	h	.1mm

PZT patches were having electrodes on both top and bottom and were connected to the high and low voltage terminals of the LCR meter. PZT patches were pasted on the flat surface of the specimens at one side by Araldite epoxy as shown in Figure 1 (b) [29-30]. It was kept at some distance away from the notch to protect it from possible damage during the crack growth.

2.3 Test setup, loads and procedure

Crack growth under cyclic loading conditions broadly depends on the type and history of the loading, geometry of the specimen/component, length of the crack and frequency of the loading [26]. All the tests on edge cracked compact tension (CT) specimen were conducted on a 25kN servo-hydraulic test system (BISS-TWI USA) at MNNIT Allahabad Prayagraj (India) as shown in Figure 2 under load control mode and frequency equal to 10 Hz.



Figure 2. A 25kN servo-hydraulic Test System

Electro-mechanical impedance were recorded with the help of Hioki make LCR meter (model IM3536) as shown in Figure 3. All tests were performed in air and room temperature. The test specimen was gripped with the help of a pin in the gripper, as shown in Figure 4. This eliminates the chances of bending of the specimen and ensures a Mode-I loading conditions. The propagation of the crack was measured by a crack

opening displacement gauge (COD) which was placed at the mouth of the notch as shown in Figure 4 and a data acquisition system integrated with the machine stores data at every point of the test [19-20]. Compact tension (CT) specimens of AA-5083 aluminum alloy were tested with stress ratio equal to 0.1 under different loading conditions.



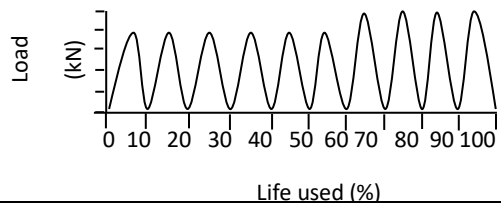
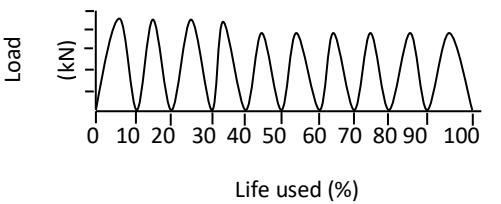
Figure 3. LCR meter (HIOKI IM 3538)



Figure 4 Specimen gripping on the test system with COD

Fatigue crack growth is significantly influenced by load history. During variable amplitude loading, crack growth rates may either increase or decrease depending on the specific loading sequence. The block loadings such as a High-Low and Low-High amplitude load sequences as shown in Table 4 were studied. Two step block-loading was considered with number of cycles under lower and higher stress amplitude equal to 60% and 40% of the number of cycles till fracture for CAL with same stress amplitude. The stress under block loading was increased (for Low-High) and decreased (for High-Low) by 12.5% as shown in Table 4.

Table 4 Block loading conditions for AA-5083 and Al-6061

	Loading	F_{max}	F_{min}	R
Lo-High		4kN 4.5kN	0.4kN 0.45kN	0.1
High-Lo		4.5kN 4kN	0.45kN 0.4kN	0.1

The life determined under constant amplitude load was used to determine the number of cycles under low and high loading conditions for the case of block loading conditions. Three tests were performed on each testing conditions and average of three tests was considered as a life for that particular condition. LCR was used to supply the alternating voltage and to measure the corresponding EM admittance signatures (Conductance and Susceptance) in the sweep measurement mode. Frequency range of 100-180 kHz was used for testing, at 6 intervals of loading cycles. The data storage system was integrated with LCR meter (Figure 3), which stores the admittance signatures data with the help of a customized software [32].

2.4 Damage assessment with the help EMI technique.

The assessment of damage under different kind of loading conditions was monitored with respect to the healthy state of the specimen. Initially, the admittance of a healthy specimen was monitored; afterward different cyclic load at different interval was applied and damage was assessed till fracture of the specimen. At the beginning of the experiment, the crack length of 12 mm was taken for base admittance signature. Total four signatures were taken corresponding to crack lengths of 12 mm, 13.5 mm, 15.5 mm and 18 mm respectively. Thereafter, conductance versus frequency plot was drawn to explore the possible application of EMI technique in determination of damage under different cyclic loading conditions.

3. Results and Discussions

First of all results of crack propagation and fracture of aluminum alloy Al-5083 under constant amplitude and block loading conditions are presented. Thereafter, implementation of Electro-mechanical impedance technique under these conditions is presented.

3.1 Crack growth investigation of Al-5083 with a COD gauge

Compact tension (CT) specimens of AA-5083 aluminum alloys were tested under loading conditions as given in Table 4. Three tests were performed for each testing conditions. S_1 , S_2 , and S_3 are sample number one, two, and three respectively. Tables 5 present the number of cycles till failure for AA-5083 aluminum alloy at constant amplitude loading (CAL) and block loading (BL) conditions as per Tables 2 and 3 respectively.

Table 5 Number of cycle till failure for AA-5083 aluminum alloy for CAL and BL conditions

Loading Condition (Max. Load)	R-ratio	No of cycles till fracture			Average life	Std.	C. Level
		S_1	S_2	S_3			
CAL-3.0 kN	0.1	41750	44590	43200	43180	1420	3527

CAL-4.0 kN	0.1	24556	23659	25909	24708	1132	2813
CAL-4.5 kN	0.1	17002	18395	17690	17695	696	1730
CAL-5.0 kN	0.1	13300	12900	13680	13293	390	969
BL (Lo-Hi) (4 kN-4.5 kN)	0.1	21546	21700	20190	21078	973	1970
BL (Hi-Lo) (4.5 kN - 4 kN)	0.1	22450	21460	23300	22403.3	920	2285



Figure 5 (a) A propagated crack in specimen during loading

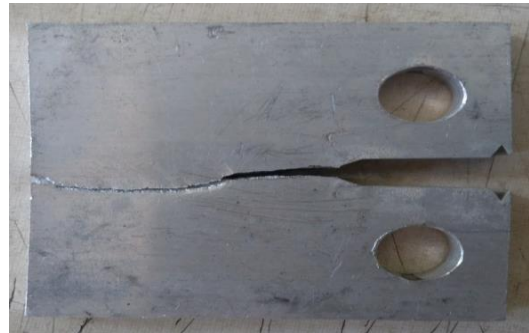


Figure 5 (b) Fractured sample

The crack length at the start for all cases was 12 mm whereas it was 24 mm at the time of fracture. Figure (5 (a)) shows a propagated crack in the CT-specimen during loading and Figure (5(b)) shows the fractured sample. Under CAL, life of the specimen decreases with increase in stress amplitude and under block loading conditions life is more for Hi-Lo sequence in comparison to Lo-Hi (Tables 5)

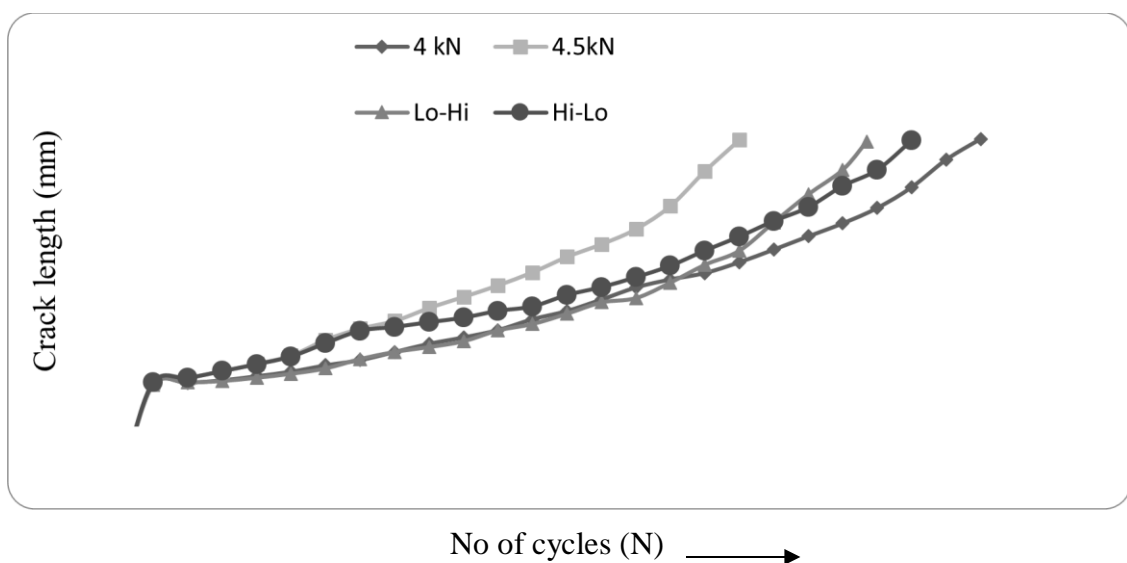


Figure 6. Crack growth versus number of cycles for AA-5083

Figure (6) shows the graph between crack length and number of cycles under constant amplitude and block loading conditions for Al-5083. Results show that crack growth rate is strongly influenced by the loading magnitude. Crack growth rate accelerates when a Low-High load sequence is followed e.g. 4.5 kN maximum load was applied after 4 kN of load but when small load amplitude was applied after bigger load amplitude (High-Low sequence) crack growth retards and approximately approached to the crack growth curve for CAL with maximum stress equal to 4.0 kN. These behaviors are as per reported in the literature.

3.2 Crack growth investigation of Al-5083 with the help of EMI signature

The real part of admittance signature was used as a damage quantifier due to its higher sensitivity compared to imaginary part of admittance signature [31]. In this study the frequency range selected for crack detection is 50 kHz to 180 kHz to minimize effects of bonding and other environmental condition at higher frequency range. Specimens were loaded as per the loading conditions shown in Table 4 till fracture. Specimen with initial crack length of 12 mm was taken for reference or baseline admittance signature. Total six signatures were taken corresponding to crack lengths of 12 mm, 13.5 mm, 15.5 mm, 18 mm, 21 mm and 24 mm.

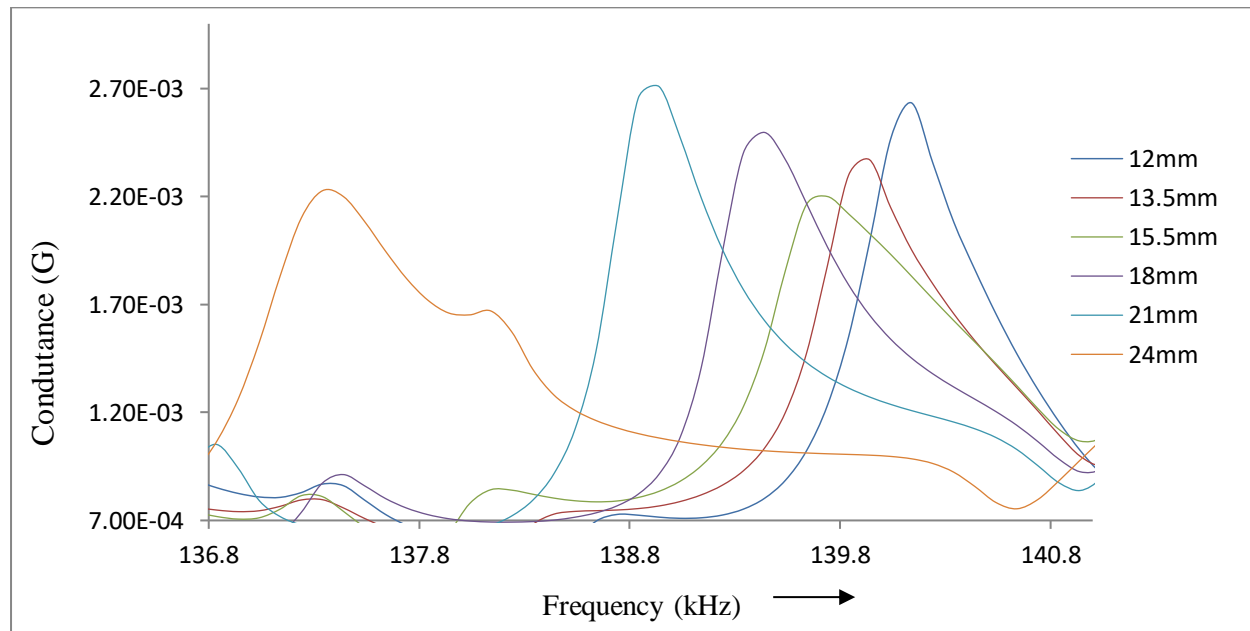


Figure 7 - ACS versus frequency for CAL - 4 kN condition (136 kHz- 141 kHz)

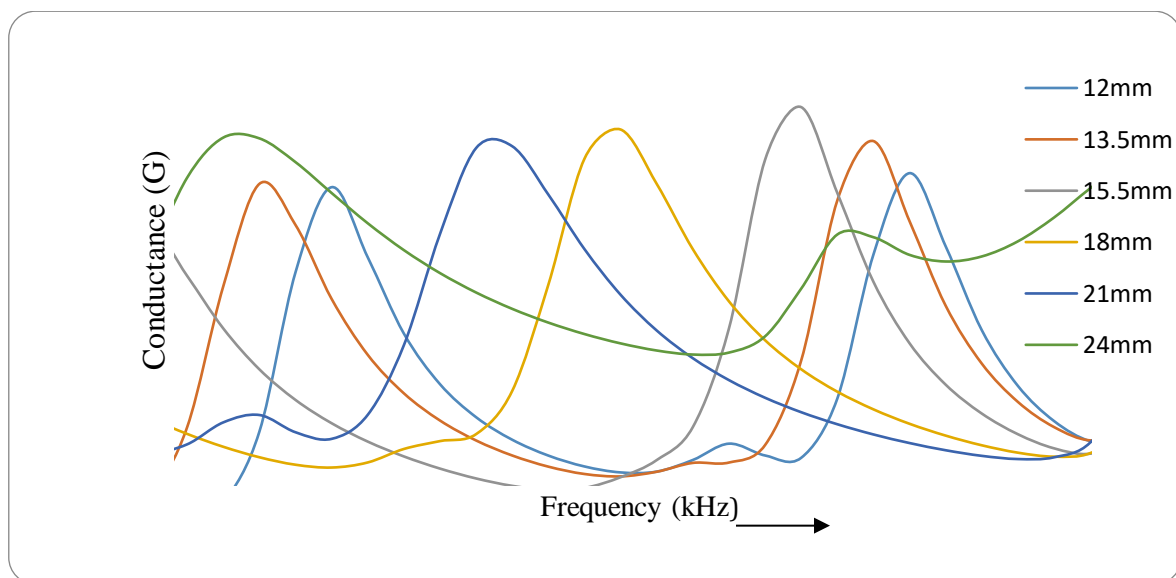


Figure 8 - ACS vs Frequency for 4.5 kN CAL condition (136 kHz- 141 kHz)

The plots of active conductance signature (ACS) of specimen were recorded at different damaged stages (length of the crack) against frequency and are presented in Figures ((7)-(10)) for AA-5083 aluminium alloy. The corresponding crack length and shift in frequency at different loading cycles for all conditions were obtained in the frequency range of 136 – 141 kHz. Leftward horizontal movement of the conductance peak i.e. reduction in resonance frequency gives useful insight for fatigue crack propagation [33]. Gradual and continuous horizontal leftward shift of the resonance peak at different loading conditions was observed. This behaviour was obtained for all cyclic loading conditions e.g. for both constant amplitude and block loading conditions. Initial shift is smaller indicating smaller damage whereas during the last stage (near the fracture point) the shift is bigger. Therefore, resonance frequency (RF) shift was quantified as a measure of damage. Shifting of RF depends on loading magnitude and corresponding crack growth rate. The results of crack growth and EMI analysis are presented in Table 6 for AA-5083 alloy.

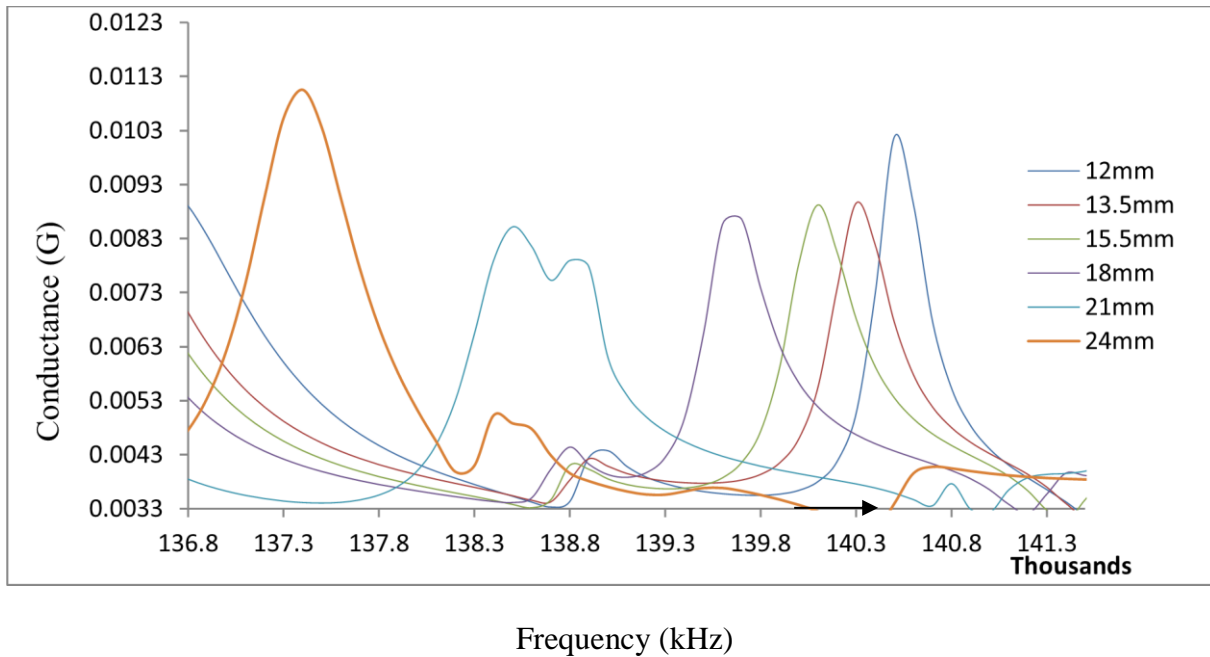


Figure 9 – ACS vs Frequency for Lo-Hi loading condition (136kHz- 141kHz)

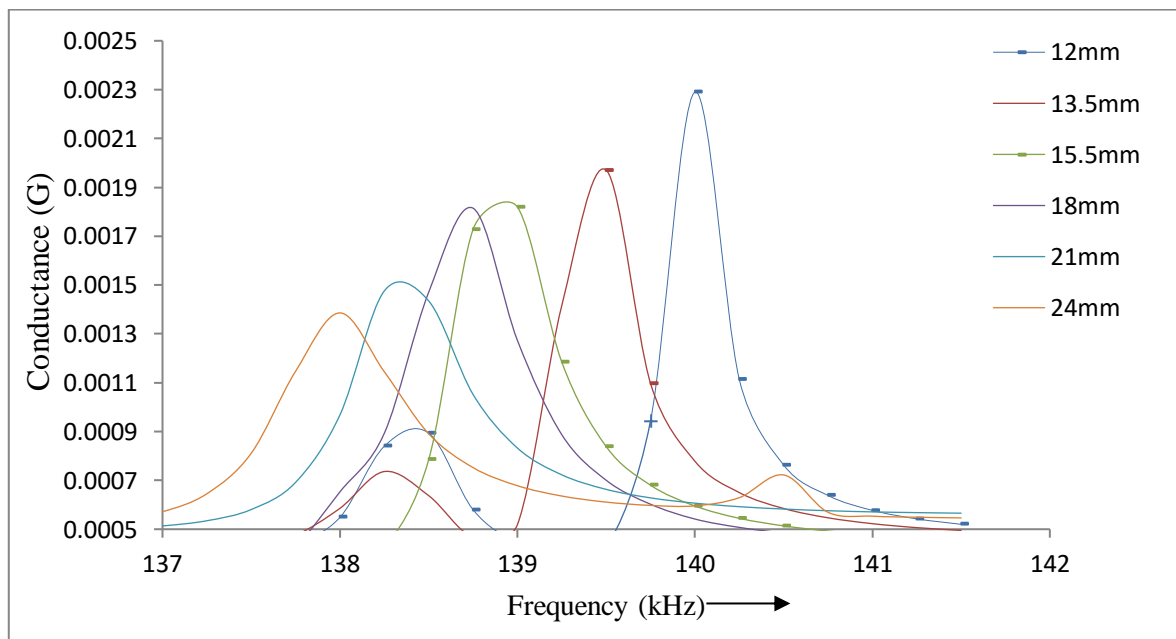


Figure 10 – ACS vs Frequency for Hi-Lo loading condition (136 kHz- 141 kHz)

In Table (6), the ΔF is the shift in resonance frequency between two consecutive crack growths and RF shift is shift of resonance frequency from initial crack length. Both of these values increase with increase in the crack growth as stiffness of the material decreases with increase in crack. The rate of shift is initially small which increases with increase in the crack growth or decrease in the stiffness e.g. for CAL of maximum stress 4 kN, for a crack growth from 12 mm to 13.5 mm the shift in resonance frequency is only 200 kHz whereas between 21 mm to 24 mm, it is 2400 kHz. For bigger CAL load of 4.5 kN, this shift is more in comparison to smaller CAL of 4 kN. For 4.5 kN maximum load CAL conditions, these corresponding values are 300 kHz and 2900 kHz. In a Low - High block loading condition starting with 4 kN maximum load followed by 4.5 kN maximum load, initial shift in resonance frequency i.e. from 12 mm crack length to 13.5 mm crack length, is 200 kHz which was same for CAL with maximum load of 4 kN. In later stages, when higher load was applied resonance shift turns towards CAL of 4.5 kN maximum load.

Table 6 Test results of crack growth and EMI for AA-5083 tested under the conditions as per Table 7

Max. Load	Crack length a	No. of cycles N	Resonance frequency F	da/dN	ΔK	Life used (%)	ΔF kHz	R.F. shift
CAL 4 kN	12	875	140433	0.0002543	15.2851	3	0	0
	13.5	7983	140267	0.0004083	17.785	28	200	200
	15.5	12917	139900	0.0006063	19.585	45	300	500
	18	17217	139500	0.0008033	21.755	68	500	1000
	21	21727	138933	0.001109	26.579	88	600	1600
	24	24067	138267	0.0020953	32.109	96	800	2400
CAL 4.5 kN	12	760	140233	0.000406	16.33	3	0	0
	13.5	5533	140000	0.000534	19.25	27	300	300
	15.5	9233	139700	0.0008303	21.31	46	400	700
	18	12233	139133	0.0011203	24.2	66	600	1300
	21	15767	138433	0.001582	28.89	84	700	2000
	24	17433	137567	0.0025737	35.38	95	900	2900
BL Lo - Hi 4 kN followed by 4.5 kN	12	873	140500	0.0002567	15.12	5	0	0
	13.5	7800	140267	0.0004195	17.8	23	200	200
	15.5	12783	139867	0.000624	20.56	51	400	600
	18	16667	139333	0.0009017	24.6	74	500	1100
	21	19667	138700	0.0012556	30.02	88	700	1800
	24	21450	137933	0.0023933	36.56	95	900	2700
BL Hi - Lo 4.5 kN followed by 4 kN	12	817	140367	0.0004013	16.51	4	0	0
	13.5	4887	140167	0.00056	19.25	20	200	200
	15.5	9900	139733	0.0008636	23.15	42	450	650
	18	15667	139200	0.0011235	25.89	69	600	1250
	21	19733	138533	0.0014127	28.98	86	700	1950
	24	22067	137733	0.0023997	34.24	94	900	2800

To co-relate crack growth rate with shift in resonance frequency, the crack length and shift in resonance frequency (RF) are plotted against percentage of life cycles in Figures (11a) and Figure (11 b) respectively. Both the plots are showing similar trend and the slopes of the curves vary in a same way. By comparison, it can be said that small slope of the curve between RF and % of life during 0-30% of life cycles gives indication of slow crack growth. In 30-80% segment, slope of curve increases which give indication of increase in crack growth. Beyond the 80% of life cycles slope of curve increases rapidly up-to the fracture. Figure 9 shows the shift in resonance frequency plotted against the percent life cycles for 4kN, 4.5kN, L-H,

and H-L block loading conditions.

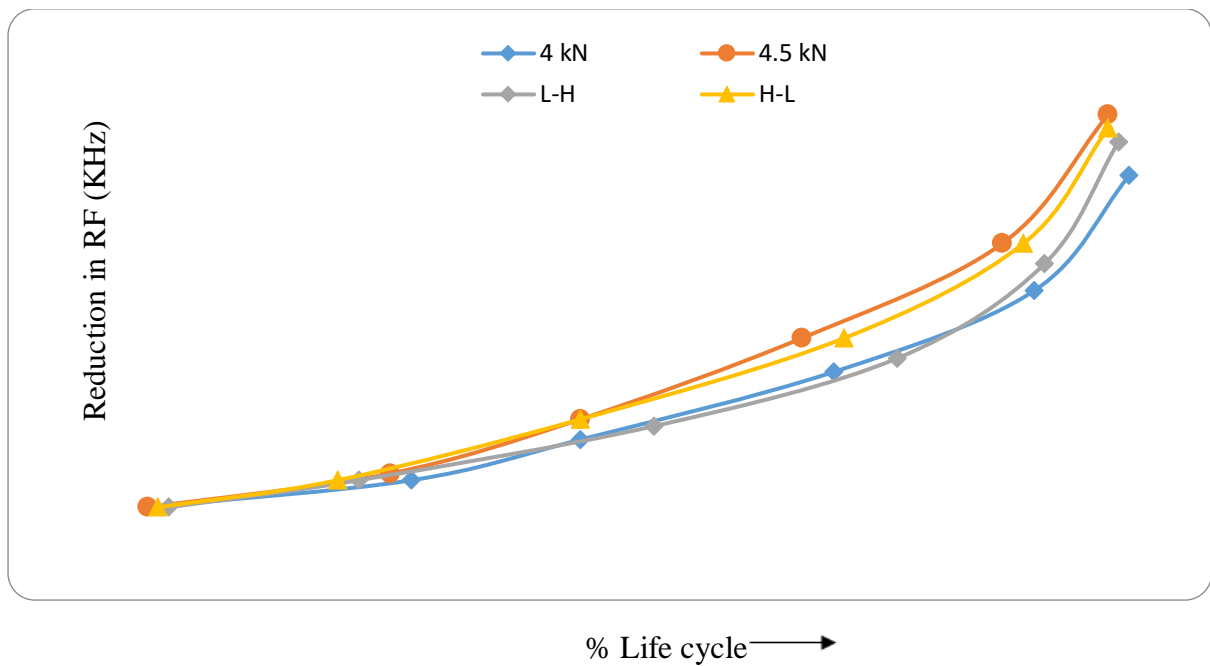


Figure 11 (a) Reduction in RF versus Life cycles for different loading conditions

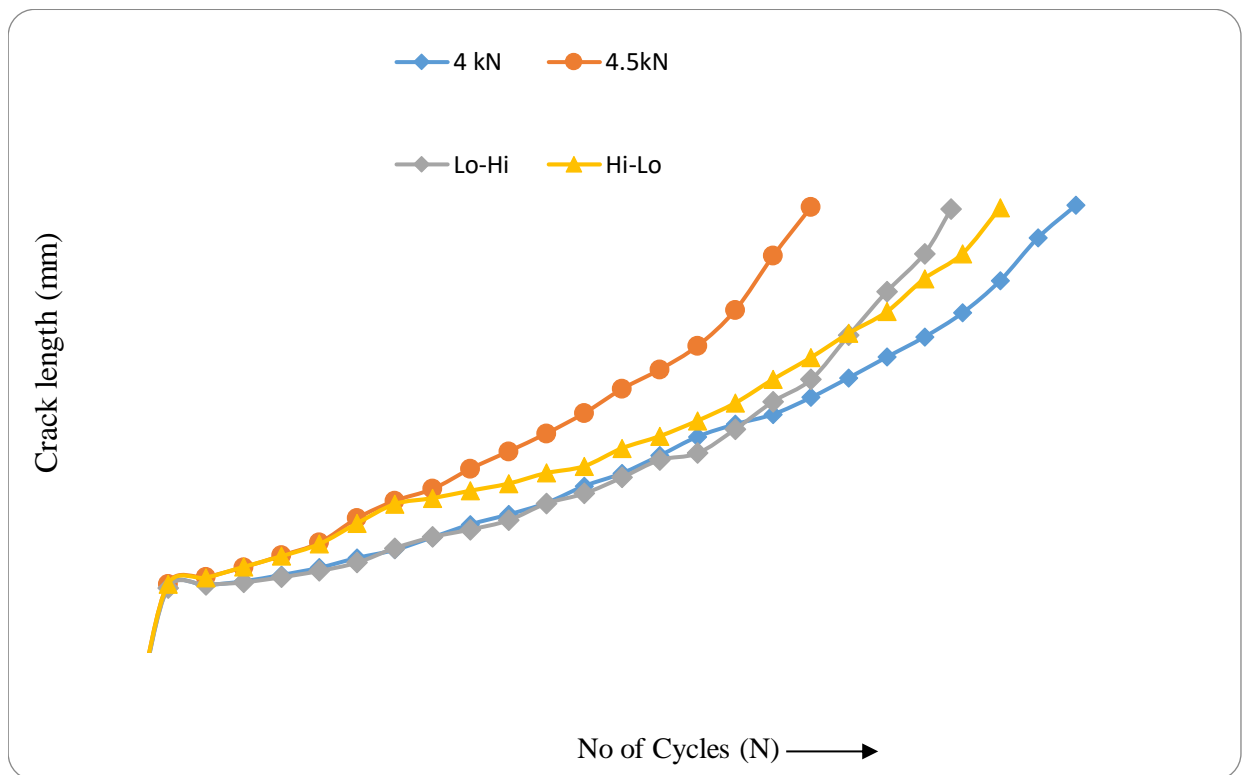


Figure 11 (b) Crack lengths versus No of cycles for different loading conditions

The plotted curves show that shift in resonance frequency with percent of life cycles has similar trend as crack length growth with number of cycles. Shift in resonance frequency as shown in Figure 11 (b) depends

upon the loading amplitude and sequence of loading. In case of L-H loading sequence, an acceleration of shift in resonance frequency was observed as life cycles progresses. For the H-L loading sequence, a retardation of shift in RF was observed as life cycles progresses, Figure 11 (a). The trend is very much same as shown in Figure 11 (b) for Hi-Lo block loading. Therefore, the shift in resonance frequency can be a good measure to determine damage or crack growth in either constant amplitude or block loading conditions.

4. Conclusions

The following conclusions are derived from the application of EMI technique on determination of damage under different block loading conditions and an overload loading condition:

1. EMI technique can be used for co-relating crack growth rate, retardation of crack growth and acceleration of crack growth under block loading conditions.
2. Gradual and continuous horizontal leftward shifting of the resonance peak was observed as a damage identifier. Shifting of resonance peak frequency (RF) depends on loading the magnitude of maximum load and crack growth rate.
3. The peaks from a higher frequency range are used for characterization due to their higher sensitivity. The shift of resonance peak frequency depends upon material, loading amplitude and sequence. For AA-5083 aluminum alloy, frequency range of 136-141 kHz was found suitable as damage identifier.
4. For constant amplitude loading, Low-High and High-Low block loading conditions, the curves plotted between crack length versus percent of total life and shift in resonance frequency and percent of total life have similar trends. Thus, EMI based shift in resonance frequency versus percent of total life cycle provides same information as was available with conventional crack length versus percent of total life cycle curves. But the advantages of quick, reliable and cost effective EMI technique may provide information about the instantaneous damage. Remote access and monitoring is also possible with the EMI technique.
5. For block loads the reduction in resonance frequency with percent of total life cycles has similar trend as a plot between crack length growth and number of cycles. Reduction in resonance frequency depends upon the loading amplitude and sequence of loading. For the case of L-H loading sequence, an acceleration of reduction in resonance frequency observed as life cycles progress. For the H-L loading sequence, a retardation of reduction in resonance. For the case of block loading, in 0-40% of total life cycles slope of the curve was small and total shift in RF was 0.5 kHz. In 40-80% slope of curve increasing, indication of crack growth increase. Beyond the 80% of life cycles slope of curve high and total reduction in RF 2.8 kHz.

5. References

- 1 Sun, F. P., Chaudhry, Z., Rogers, C. A., Majmundar, M. and Liang, C. (1995) "Automated Real-Time Structure Health Monitoring via Signature Pattern Recognition", edited by I. Chopra, Proceedings of SPIE Conference on Smart Structures and Materials, San Diego, California, Feb.27-Mar1, SPIE vol. 2443, pp. 236-247.
- 2 Ayres J. W., Lalande F., Chaudhry Z., Rogers C. A., 1998, "Qualitative impedance-based health monitoring of civil infrastructures", *Smart Materials and Structures*, 7 (5), pp. 599-605.
- 3 Park G., Cudney H.H., Inman D. J., 2000a, "Impedance-based health monitoring of civil structure components", *Journal of Infrastructure System, ASCE*, 6 (4), pp. 153-160.
- 4 Park G., Cudney, H.H., Inman D. J., 2000b, "An integrated health monitoring techniques using structural impedance sensors", *Journal of Intelligent Material Systems and Structures*, 11, pp. 448-455.
- 5 Soh C.K., Tseng K.K.H., Bhalla S., Gupta, A., 2000, "Performance of smart piezoceramic patches in health monitoring of a RC bridge", *Smart Materials and Structures*, 11 (4), pp. 246-257.
- 6 Lopes V., Park G., Cudney H. H., Inman D. J., 1999, "Smart structures health monitoring using artificial neural network", *Proceedings of 2nd International Workshop on Structural Health Monitoring*, edited by F. K. Chang, Stanford University, Stanford, CA, September 8-10, pp. 976-985.
- 7 Abe M., Park G., Inman D. J., 2002, "Impedance-based monitoring of stress in thin structural members", *Proceeding of 11th International Conference on Adaptive Structures and Technologies*, October 23-26, Nagoya, Japan, pp. 285-292.
- 8 Giurgiutiu V., Zagrai A. N., 2002, "Embedded self-sensing piezoelectric active sensors for on-line structural identification", *Journal of Vibration and Acoustics, ASME*, 124, pp. 116-125.

- 9 Isabela Iuriko Campos Maruo, Guilherme de Faria Giachero, Valder Steffen Júnior, Roberto Mendes Finzi Neto, Electromechanical Impedance – Based Structural Health Monitoring Instrumentation System Applied to Aircraft Structures and Employing a Multiplexed Sensor Array, *Journal Aerospace Technology Management*, São José dos Campos, 7 (3), (2015), 294-306.
- 10 Kevin Fan-Ying Tseng, Liangsheng Wang, Smart piezoelectric transducers for in situ health monitoring of concrete. *Smart Materials and Structures* 13(5):1017. (2004).
- 11 Park, S., Yun, C.B., Roh, Y. and Lee, J.J. (2006), "PZT-based Active Damage Detection Techniques for Steel Bridge Components", *Smart Materials and Structures*, Vol. 15, pp. 1734-1746.
- 12 W. Yan, W. Q. Chen, C. W. Lim, and J. B. Cai, Application of EMI Technique for Crack Detection in Continuous Beams Adhesively Bonded with Multiple Piezoelectric Patches. *Mechanics of Advanced Materials and Structures*, 15:1-11, 2008.
- 13 Zagrai, Andrei N., and Victor Giurgiutiu. "Electro-mechanical impedance method for crack detection in thin plates." *Journal of Intelligent Material Systems and Structures* 12.10 (2001): 709-718.
- 14 Yee Yan Lim and Chee Kiong Soh, Fatigue life estimation of a 1D aluminum beam under mode-I loading using the electromechanical impedance technique', *Smart Materials and Structures*, vol. 20, no. 12. (2011).
- 15 Fabricio G. Baptista, Danilo E. Budoya, Vinicius A. D. de Almeida and Jose Alfredo C. Ulson, An Experimental Study on the Effect of Temperature on Piezoelectric Sensors for Impedance-Based Structural Health Monitoring. *Sensors* 14, 1208-1227, 2014.
- 16 Mateusz Rosiek, Adam Markowitz, and Tadeusz Uh, Electro-mechanical impedance based SHM system for aviation applications. *Key Engineering Materials* Vol. 518 (2012) pp 127-136.
- 17 Bhalla, S. (2004), "A Mechanical Impedance Approach for Structural Identification, Health Monitoring and Non-Destructive Evaluation Using Piezo-Impedance Transducer" Ph.D. Thesis, Nanyang Technological University, Singapore.
- 18 Palomino, Lizeth Vargas, et al. "Impedance-based health monitoring and mechanical testing of structures." *Smart Structures and Systems* 7.1 (2011): 15-25.
- 19 Yee Yan Lim & Chee Kiong Soh, Electro-Mechanical Impedance (EMI)-Based Incipient Crack Monitoring and Critical Crack Identification of Beam Structures. *Research in Nondestructive Evaluation* 25:82-98, 2014. [up to ch-2]
- 20 Ngiau Christopher and Daniel Kujawski, 2001, "Effects of small amplitude cycles on fatigue crack initiation and propagation in 2024-T351 Aluminum", *International Journal of Fatigue*, 23, pp.807-815.
- 21 Memon Iqbal Rasool, Xing Zhang, Deyu Cui, 2002, "Fatigue life prediction of 3-d problems by damage mechanics with two-block loading", *International Journal of Fatigue*, 24, pp. 29-37.
- 22 Pinho-da-Cruz J. A. M., Ferreira J. A. M., Costa J. D. M., Borrego L. F. P., 2003, Fatigue analysis of thin Al Mg si welded joints under constant and variable amplitude block loadings", *Thin-Walled Structures*, 41, pp. 389-402.
- 23 Rodopoulos Chris A., and Kermanidis Alexis Th., 2007, "Understanding the effect of block-overloading on the fatigue behaviour of 2024-T351 Aluminium alloy using the fatigue damage map", *International Journal of Fatigue*, 29, pp. 276-288.
- 24 Borrego L.P., Ferreira J. M., Costa J. M., 2008, "Partial crack closure under block loading", *International Journal of Fatigue*, 30, pp.1787-1796.
- 25 Carvalho A.L.M., Martins J.P., Voorwald H.J.C., 2009, "Fatigue damage accumulation in aluminum 7050-T7451 alloy subjected to block programs loading under step-down sequence", *Procedia Engineering*, 2, pp. 2037-2043.
- 26 Fleck N. A., 1985, "Fatigue crack growth due to periodic underloads and overloads", *Acta Metallurgica*, 33, pp. 1399 - 1354.
- 27 Makabe C., Purnowidodo A., McEvily A.J., 2004, "Effects of surface deformation and crack closure on fatigue crack propagation after overloading and under-loading", *International Journal of Fatigue*, 26, pp.1341-1348.
- 28 Smith K.V., "Application of the dissipation energy criterion to predict fatigue crack growth of type 304 stainless steel following a tensile overload", *Engineering Fracture Mechanics*, 78(18), 2011, pp. 3183-3195.
- 29 Bhalla, Suresh, and Chee-Kiong Soh. "Electro-mechanical impedance technique for structural health monitoring and non-destructive evaluation." *National workshop on structural health*

- monitoring, non-destructive evaluation and retrofitting of structures. Indian Institute of Technology Delhi. 2008.
- 30 Soh, Chee- Kiong, Yaowen Yang, and Suresh Bhalla, eds. Smart materials in structural health monitoring, control and biomechanics. Springer Science & Business Media, 2012
 - 31 Babu, K. K., Panneerselvam, K., Sathiya, P., Haq, A.N., Sundarrajan, S., Mastanaiah, P. and Murthy, C.V.S., Experimental Investigation on friction stir welding of Cryorolled AA2219 aluminum alloy joints, Surface Review and Letters, 24.1 (2017),1750001.
 - 32 Lim, Y. Y. and Soh, C.K., Estimation of fatigue life using electromechanical impedance technique. Proc SPIE 7647, Sensors and Smart Structures Technologies for Civil, Mechanical, and Aerospace Systems (2010), 764722 (32 March 2010).
 - 33 J.W.Ponton, G M C Lee, Crack-opening displacement as a method of measuring crack length in compact-tension specimens, Journal of Strain Analysis vol 15 No 1 1980, pp. 31-35.